PHYSICAL REVIEW E **83**, 030101(R) (2011)

Predictability of anomalous transport on lattice networks with quenched disorder

Peter K. Kang,[1] Marco Dentz,[2] and Ruben Juanes[1,*]
[1]*Massachusetts Institute of Technology, 77 Massachusetts Avenue, Building 48, Cambridge, Massachusetts 02139, USA*
[2]*Spanish National Research Council (IDÆA-CSIC), E-08034 Barcelona, Spain*

(Received 20 July 2010; published 4 March 2011)

We study stochastic transport through a lattice network with quenched disorder and evaluate the limits of predictability of the transport behavior across realizations of spatial heterogeneity. Within a Lagrangian framework, we perform coarse graining, noise averaging, and ensemble averaging, to obtain an effective transport model for the average particle density and its fluctuations between realizations. We show that the average particle density is described exactly by a continuous time random walk (CTRW), and the particle density variance is quantified by a novel two-particle CTRW.

DOI: 10.1103/PhysRevE.83.030101 PACS number(s): 05.60.Cd, 05.10.Gg, 05.40.Fb, 92.40.Kf

Transport of individual agents on networks leads to the emergence of collective dynamics that govern many processes in nature and society, such as traffic patterns [1], evacuation systems [2], bubble microfluidic devices [3], cell motility in dense actin filament networks [4], and flow through geologic fractures [5]. Recent analyses have led to key advances in the theory of transport on networks, including an understanding of the conductance between two arbitrarily chosen nodes in scale-free or Erdős and Rényi networks [6], and spreading behavior by means of diffusive random walks [7,8]. However, predictive theories of the aggregate transport behavior are still in their infancy and are likely to be one of the next frontiers in network science [9]. This has proven challenging because the dynamics depend on network topology as well as on the underlying transport mechanisms, such as the balance between advection and diffusion [10], or diffusion and reaction [11,12]. Another fundamental challenge is that the detailed properties of the network are often inaccessible to direct observation. As a result, transport must be understood in a stochastic framework, and characterizing the system requires not only estimating the expected evolution, but also evaluating its predictability—the confidence with which a prediction can be made—at the level of individual agents [13] and also in terms of the mean-field behavior [14].

Here, we show that the ensemble behavior of kinetic particle transport in a lattice network with quenched disorder in particle velocity can be described exactly by a continuous time random walk (CTRW) [15–18]. This provides an exact coarse-grained model for the *expected value* of particle density in space and time, thereby advancing CTRW not only as an effective modeling approach [5,19], but also as a stochastic description that emanates from proper upscaling of the microscale [20].

The central result of this Rapid Communication is an explicit stochastic averaging of the quenched disorder that allows for the systematic quantification of the *sample-to-sample fluctuations* in particle density about the expected behavior. Fluctuation quantification for random walks has been addressed previously in annealed random environments [21,22]. While some annealed and quenched disorder scenarios lead to the same average behavior (CTRW), they exhibit different fluctuation dynamics. Although much of the mean behavior of our model can be understood from a one-dimensional (1D) system [23], the fluctuation behaviors for 1D and two-dimensional (2D) systems are fundamentally different. Here, we address the predictability of random walks in a quenched random environment by developing a novel two-particle process that exactly describes the variability in particle density among equiprobable realizations of the network's quenched disorder. Our theoretical model of the particle density variance takes a form that is reminiscent of CTRW, and, therefore, we coin it two-particle CTRW. This result sheds light on the spatiotemporal characteristics of uncertainty propagation and the predictability of transport through a network whose properties are unconditioned to hard data.

We consider a lattice network consisting of two sets of parallel equidistant intersecting links: one set at an angle $-\alpha$ and the other at an angle $+\alpha$ with respect to the x axis [Fig. 1(a)]. We assign i.i.d. random particle velocities $v \geqslant 0$ to each link. Different values of particle velocity are assumed to be the result of microscale processes, such as different conductance or adsorption rate. In particular, our model is an analog for transport through a fracture network

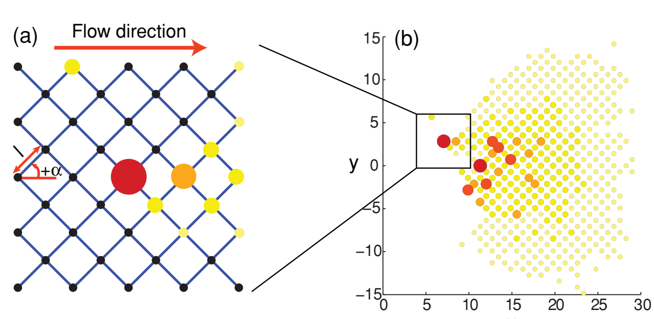

FIG. 1. (Color online) (a) Schematic of the lattice network considered here, with two sets of links with orientation $\{-\alpha,+\alpha\}$ with respect to the x axis, and lattice spacing $l = 1$. Each network realization exhibits quenched disorder in the particle velocity, with link velocities determined from an independent and identically distributed (i.i.d.) process $p_v(v)$. (b) Representation of transport through the network from particles released at the origin at $t = 0$. Shown is the particle density (represented by circle size) at $t = 30$ for a single realization with $\beta = 1.5$. The random process generating velocity disorder induces large fluctuations in the particle density between realizations.

*juanes@mit.edu

with homogeneous hydraulic properties (fracture spacing and aperture) but with chemical heterogeneity. Due to adsorption, the mean particle velocity within a link is lower than the fluid velocity by a retardation factor $R = 1 + k$, where the coefficient k is a measure of adsorption strength. Our analytical developments are valid for any velocity distribution $p_v(v)$, but in the simulations, we employ a one-sided truncated power law distribution, $p_v(v) = v^{\beta-1}\exp(-v/v_c)/[\Gamma(\beta)v_c^{\beta}]$, where β is the power law exponent, $v_c = 1$ is the characteristic value of the velocity for the exponential cutoff, and Γ denotes the Γ function. The set of all realizations of the quenched random network generated in this way form a statistical ensemble that is stationary and ergodic.

We study the spatiotemporal evolution of particles released instantaneously at the origin [Fig. 1(b)]. For a given realization, an individual particle will advance through the network moving along links with fixed random velocities. At each node, it has probability λ to move diagonally upward and probability $1-\lambda$ to move downward. For an effective transport description on an observation scale L much larger than the link length l, the detailed particle positions within the links are not needed. Thus, we coarse-grain transport and record particle positions only at nodes. The Langevin equations describing particle evolution are as follows:

$$x_{n+1} = x_n + l\cos\alpha, \qquad y_{n+1} = y_n + \xi_n l \sin\alpha, \tag{1a}$$

$$t_{n+1} = t_n + \tau(\mathbf{x}_n,\xi_n), \tag{1b}$$

where the noise $\xi_n \in \{-1,+1\}$ is distributed according to a two-valued Dirac δ function $p_{\xi_n} = (1-\lambda)\delta(\xi_n+1) + \lambda\delta(\xi_n-1)$. The Lagrangian velocity $v(\mathbf{x}_n,\xi_n)$ at the $(n+1)$th step at node at $\mathbf{x}_n$ depends on the noise ξ_n. The quenched random velocity is mapped onto the quenched random transition time between nodes, $\tau(\mathbf{x}_n,\xi_n) = l/v(\mathbf{x}_n,\xi_n)$. At a given time t, a particle is assigned to node $\mathbf{x}_n$ as long as $t < t_{n+1}$. Thus, τ is the transition time between nodes or, alternatively, the waiting time at a node. The transition times between nodes are fixed but independent, and their one point distribution $\psi(\tau)$ is obtained from the velocity distribution $\psi(\tau) = l\tau^{-2}p_v(l/\tau) \sim \tau^{-(1+\beta)}$. The system of discrete Langevin equations (1) describes coarse-grained particle transport in a single realization of the network. The particle position at a given time t is $\mathbf{x}_{n_t}$, where n_t denotes the renewal process that describes the number of steps needed to reach time t following Eq. (1b), that is, $n_t = \max\{n | t \geqslant t_n\}$.

We characterize transport in terms of the propagator $P(\mathbf{x},t)$ of the initial impulse, that is, the probability density of finding a particle at position $\mathbf{x}$ at time t, which is given in terms of the particle trajectories $\mathbf{x}_{n_t}$ as

$$P(\mathbf{x},t) = \langle \delta(\mathbf{x} - \mathbf{x}_{n_t})\rangle, \tag{2}$$

where the angular brackets $\langle\cdot\rangle$ denote noise averaging over all particles. Note that the Dirac δ is the limit of a discrete density for $L \gg l$.

We solve the transport problem in a single disorder realization by particle tracking using Eq. (1). The simulated particle densities display large sample-to-sample fluctuations [Fig. 2(a)]. By averaging over a sufficient number of realizations, we obtain the mean particle density $\overline{P}(\mathbf{x},t) = \overline{P(\mathbf{x},t)}$, where the overbar $\overline{(\cdot)}$ denotes ensemble averaging over all

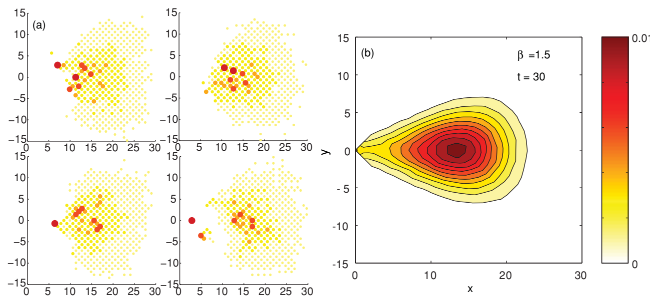

FIG. 2. (Color online) (a) Particle density at $t = 30$ for four different realizations of quenched disorder in the velocity field. Each velocity field is generated using the one-sided truncated power law distribution with the same value of the exponent $\beta = 1.5$. The disparity in the spatial distributions of particle density illustrates the need for quantifying fluctuations among realizations. (b) Mean particle density obtained by ensemble averaging, which displays a non-Gaussian shape even for long simulation times. We simulated 10^4 realizations and 10^4 particles per realization.

realizations. The mean particle density exhibits a skewed spatial distribution, which migrates and spreads with time without ever approaching the Gaussian shape characteristic of normal (Fickian) transport [Fig. 2(b)]. Average transport is anomalous in the sense that the mean square displacement (MSD), $\langle \Delta x^2\rangle$, does not scale linearly with time.

In the following, we develop a stochastic description of mean particle density and particle density variance among realizations. To derive the mean behavior, we observe that the ensemble average over Eq. (2) can be written as

$$\overline{P}(\mathbf{x},t) = \sum_{n=0}^{\infty} \langle \delta(\mathbf{x}-\mathbf{x}_n)\overline{\delta_{n,n_t}}\rangle, \tag{3}$$

where $\delta_{i,j}$ denotes the Kronecker δ. The statement $n = n_t$ encoded in δ_{n,n_t} is equivalent to the statement $0 \leqslant t - t_n < \tau(\mathbf{x}_n,\xi_n)$. Thus, the probability distribution $\overline{\delta_{n,n_t}}$ of the renewal process n_t is

$$\overline{\delta_{n,n_t}} = \int_0^t dt'\, \overline{\delta(t'-t_n)}\;\; \overline{I_{[0,\tau(\mathbf{x}_n,\xi_n)]}(t-t')}, \tag{4}$$

with the indicator function $I_{(0,\tau)}(t)$ being 1 if $t \in (0,\tau)$ and 0 otherwise. Taking the average, using the distribution $\psi(\tau)$ of transition times, and substituting Eq. (4) in Eq. (3), gives

$$\overline{P}(\mathbf{x},t) = \int_0^t dt' \sum_{n=0}^{\infty} \overline{P}_n(\mathbf{x},t)\Psi_1(t-t'), \tag{5a}$$

where we defined $\overline{P}_n(\mathbf{x},t) \equiv \langle \delta(\mathbf{x}-\mathbf{x}_n)\overline{\delta(t-t_n)}\rangle$ and $\Psi_1(\tau) = \int_\tau^\infty d\tau'\,\psi(\tau')$, the probability that the transition time is larger than τ. The density $\overline{P}_n(\mathbf{x},t)$ satisfies the Chapman-Kolmogorov equation,

$$\overline{P}_{n+1}(\mathbf{x},t) = \int d\mathbf{x}' \int_0^t dt'\, p(\mathbf{x}-\mathbf{x}')\psi(t-t')\overline{P}_n(\mathbf{x}',t'), \tag{5b}$$

where $p(\boldsymbol{\eta}) = \langle \delta[\boldsymbol{\eta} - (\mathbf{x}_{n+1} - \mathbf{x}_n)]\rangle$. The system of equations (1) describes the particle density in the CTRW framework (e.g., Refs. [16,17]). The transition time distribution $\psi(\tau)$ is uniquely defined by the distribution of the underlying quenched disorder. This implies that the mean particle density in this quenched disorder model behaves in the same way as a corresponding annealed disorder model, for which the disorder configuration changes at each time step. Since $\psi(\tau) \sim \tau^{-(1+\beta)}$, transport is anomalous for $0 < \beta < 2$ and Fickian for $\beta > 2$ [18,24].

We now turn our attention to assessing the predictive power of this result. We have already shown that, in quenched disordered systems, sample-to-sample fluctuations can be large [Fig. 2(a)]. We choose the variance $\sigma_P^2(\mathbf{x},t) = \overline{P^2(\mathbf{x},t)} - [\overline{P}(\mathbf{x},t)]^2$ as a measure of variability among realizations. The mean square density $\overline{P^2(\mathbf{x},t)}$ can be written by using the trajectories of two independent particles $\mathbf{x}^{(i)}_{n_t^{(i)}}, i = 1,2$ as

$$\overline{P^2(\mathbf{x},t)} = \sum_{n=0}^{\infty} \langle \delta(\mathbf{x} - \mathbf{x}_n^{(1)}) \delta(\mathbf{x} - \mathbf{x}_n^{(2)}) \overline{\delta_{n,n_t^{(1)}} \delta_{n,n_t^{(2)}}} \rangle, \tag{6}$$

where we used the fact that, in our network model, the space trajectories are independent of the quenched disorder and that $\mathbf{x}_n^{(1)} = \mathbf{x}_{n'}^{(2)} = \mathbf{x}$ only if $n = n'$. The joint distribution of the renewal process n_t is

$$\overline{\delta_{n,n_t^{(1)}} \delta_{n,n_t^{(2)}}} = \int_0^t dt' \int_0^t dt'' \overline{\delta(t' - t_n^{(1)}) \delta(t'' - t_n^{(2)})} \times \overline{I_{[0,\tau(\mathbf{x},\xi_n^{(1)})]}(t - t')\, I_{[0,\tau(\mathbf{x},\xi_n^{(2)})]}(t - t'')}. \tag{7}$$

Noting that $\tau(\mathbf{x},\xi_n^{(1)})$ and $\tau(\mathbf{x},\xi_n^{(2)})$ are independent for $\xi_n^{(1)} \neq \xi_n^{(2)}$, the mean square density can be written as

$$\begin{aligned}\overline{P(\mathbf{x},t)^2} = \mathsf{p} \int_0^t dt' \int_0^t dt'' \sum_{n=0}^{\infty} \overline{P}_n^{(2)}(\mathbf{x},t';\mathbf{x},t'') \Psi_2(t-t',t-t'') \\ + (1-\mathsf{p}) \int_0^t dt' \int_0^t dt'' \sum_{n=0}^{\infty} \overline{P}_n^{(2)}(\mathbf{x},t';\mathbf{x},t'') \\ \times \Psi_1(t-t')\Psi_1(t-t''),\end{aligned} \tag{8}$$

where $\overline{P}_n^{(2)}(\mathbf{x}^{(1)},t;\mathbf{x}^{(2)},t')$ denotes the two-particle space-time density, and $\Psi_2(\tau,\tau') \equiv \int_{\max(\tau,\tau')}^{\infty} d\tau''\, \psi(\tau'')$ is the probability that the transition time is larger than the maximum of τ and τ'. The probability of sampling the same noise is $\mathsf{p} = \lambda^2 + (1-\lambda)^2$. The first term on the right side of Eq. (8) accounts for the particle pairs that arrive at position $\mathbf{x}$ and move on through the same link, which renders their transition times identical. Thus, contributions to the ensemble average come only from those particle pairs for which both transition times are larger than the maximum of the differences of the observation time and the individual arrival times at $\mathbf{x}$. The second term on the right accounts for the particle pairs that, after arriving at $\mathbf{x}$, move on through different links, which yields their transition times independent of each other.

The two-particle density $\overline{P}_n^{(2)}(\mathbf{x}^{(1)},t;\mathbf{x}^{(2)},t')$ quantifies the joint probability density of finding one particle at $(\mathbf{x}^{(1)},t)$ and another at $(\mathbf{x}^{(2)},t')$ after n steps. Using the fact that random velocities in different links are independent, we obtain

$$\begin{aligned}\overline{P}_{n+1}^{(2)}(\mathbf{x},t;\mathbf{x},t') \\ = \int d\boldsymbol{\eta} \int_0^{\min(t,t')} d\tau\, p(\boldsymbol{\eta})\psi(\tau)\overline{P}_n^{(2)} \\ \times (\mathbf{x}-\boldsymbol{\eta},t-\tau;\mathbf{x}-\boldsymbol{\eta},t'-\tau) + \int d\boldsymbol{\eta} \int d\boldsymbol{\eta}' \int_0^t d\tau \\ \times \int_0^{t'} d\tau' [p(\boldsymbol{\eta}) - \delta(\boldsymbol{\eta}-\boldsymbol{\eta}')] p(\boldsymbol{\eta}')\psi(\tau)\psi(\tau')\overline{P}_n^{(2)} \\ \times (\mathbf{x}-\boldsymbol{\eta},t-\tau;\mathbf{x}-\boldsymbol{\eta}',t'-\tau').\end{aligned} \tag{9a}$$

The first term on the right quantifies the probability that two particles reach position $\mathbf{x}$ through the same link and, thus, have the same transition time. The second term accounts for particle transitions arriving at $\mathbf{x}$ from different positions such that transition times are independent. In this case, that is, when $\mathbf{x} \neq \mathbf{x}'$, the two-particle density is simply

$$\begin{aligned}\overline{P}_{n+1}^{(2)}(\mathbf{x},t;\mathbf{x}',t') \\ = \int d\boldsymbol{\eta} \int d\boldsymbol{\eta}' \int_0^t d\tau \int_0^{t'} d\tau'\, p(\boldsymbol{\eta})p(\boldsymbol{\eta}')\psi(\tau) \\ \times \psi(\tau')\overline{P}_n^{(2)}(\mathbf{x}-\boldsymbol{\eta},t-\tau;\mathbf{x}'-\boldsymbol{\eta}',t'-\tau').\end{aligned} \tag{9b}$$

The system of equations (9) describes a two-particle CTRW that exactly quantifies the mean square density and, therefore, the particle density variance. The corresponding Langevin equations are the particle-pair ($i = 1,2$) trajectories,

$$x_{n+1}^{(i)} = x_n^{(i)} + l\cos\alpha, \quad y_{n+1}^{(i)} = y_n^{(i)} + \xi_n^{(i)} l \sin\alpha, \tag{10a}$$

$$t_{n+1}^{(i)} = t_n^{(i)} + \tau_n^{(i)}, \tag{10b}$$

where the particle-pair transition times $\{\tau^{(1)},\tau^{(2)}\}$ are distributed according to $\psi_2(\tau_n^{(1)},\tau_n^{(2)}) = \psi(\tau_n^{(1)})\delta(\tau_n^{(1)} - \tau_n^{(2)})$ if $\mathbf{x}_n^{(1)} = \mathbf{x}_n^{(2)}$ and $\xi_n^{(1)} = \xi_n^{(2)}$ and according to $\psi_2(\tau_n^{(1)},\tau_n^{(2)}) = \psi(\tau_n^{(1)})\psi(\tau_n^{(2)})$ otherwise.

Let us explain this two-particle process more plainly. Consider a pair of particles (a red particle and a blue particle) that are released simultaneously at the origin. Each particle traverses the lattice from left to right and has equal probability of moving diagonally up and diagonally down at each node. Since the two particles migrate in a directed network, each particle can traverse a link only once. If, at a given step i, the two particles traverse different links, they experience two independent waiting times, τ_i and τ_i'. In other words, when the two particles traverse different links, they sample the transition-time probability distribution *independently*. If, at a given step p of the process, the two particles traverse the same link, both particles experience *the same* waiting time for that jump, $\tau_p = \tau_p'$. Following this process, we assign, to each particle, a sequence of network positions ($\{\mathbf{x}_i\}$, $\{\mathbf{x}_i'\}$) and time intervals ($t_{i+1} - t_i$, $t_{i+1}' - t_i'$) spent at each location. We repeat this *annealed* process for many particle pairs, which we express in the paper with the Langevin equations (10). Counting the number of events when the two particles share a node (same position) during a period (same time) and using the total number of particle pairs injected as a normalization factor, allows us to determine the mean square particle density, $\overline{P^2(\mathbf{x},t)}$, and therefore, the variance $\sigma_P^2(\mathbf{x},t) = \overline{P^2(\mathbf{x},t)} - [\overline{P}(\mathbf{x},t)]^2$.

The typical spatial distribution of the variance shows that uncertainty is largest near the origin and decreases with particle travel distance [Fig. 3(a)]. The variability in transport velocities near the injection point greatly impacts the

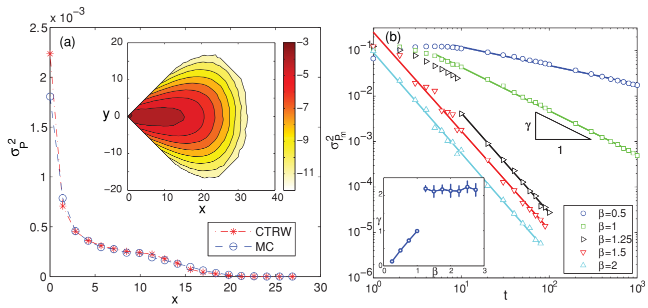

FIG. 3. (Color online) (a) Profile of the variance σ_P^2 along the x axis at $t = 30$ for a lattice with velocity disorder given by a power law exponent $\beta = 1.5$. The predictions from the two-particle CTRW simulation are obtained with 10^5 successful particle pairs. We compare these results with those obtained from Monte Carlo simulation with 10^4 quenched disorder realizations and 10^4 particles per realization. Inset: 2D spatial map of the logarithmic variance. (b) Time evolution of the variance at the point of maximum particle density, $\sigma_{P_m}^2$, showing a power law decay of the variance, $\sigma_{P_m}^2 \sim t^{-\gamma}$. Inset: dependence of γ on the power law exponent of the velocity distribution β. The results are obtained with the two-particle CTRW formulation, using 10^5 successful particle pairs per simulation.

overall plume shape, suggesting that conditioning the velocity disorder to hard data near the injection point is an effective strategy to reduce uncertainty.

An important question regarding predictability of transport is how the variance—especially, the variance where the particle density is maximum, $\sigma_{P_m}^2$—evolves in time. Simulations using the two-particle CTRW formulation show that, for the one-sided truncated power law velocity distribution, $\sigma_{P_m}^2$ follows a power law decay with time, $\sigma_{P_m}^2 \sim t^{-\gamma}$ [Fig. 3(b)]. Increasing γ implies that the predictability increases at a faster rate. The dependence of γ on the power law exponent of the velocity distribution β displays a nontrivial trend. For values $\beta \leqslant 1$, γ increases linearly with β [Fig. 3(b)]. The asymptotic exponent γ increases abruptly for values $\beta > 1$, corresponding to a transition from a situation in which the point of maximum particle density is stationary at the origin ($\beta < 1$) to one in which this point migrates away from the origin as time evolves ($\beta > 1$). Such transition also coincides with the crossover from growing to decaying probability of vanishing link velocities. The exponent γ saturates for larger values of β. The transition from anomalous to normal transport occurs at $\beta = 2$, whereas, the transition in predictability (from more predictable to less predictable transport behavior) occurs at $\beta = 1$. The transition in predictability at $\beta = 1$ is confirmed by the time evolution of the relative fluctuation $\sigma_{P_m}/\overline{P}_m$ at the point of maximum particle density. The relative fluctuation remains constant with respect to time for $\beta > 1$, and this constant value decreases with increasing β, whereas, for $\beta < 1$, the relative fluctuation increases linearly with time (not shown). These results suggest that, for our system, strong anomalous transport exhibits lower intrinsic predictability than normal transport.

Because of the relative simplicity of our transport model (particles walk on a directed lattice, and the quenched disorder in transition times is spatially uncorrelated), our annealed two-particle model is exact. Our results provide insight into the behavior of the particle density variance during transport in quenched disorder, and they also lead to much more efficient variance quantification than a Monte Carlo simulation approach. Our effective description of anomalous transport emanates not from fitting transport behavior—such as scalings of the MSD or the mean first passage time—but from rigorous upscaling of the microscale dynamics. Our theoretical results establish a foundation for developing macroscopic models of anomalous transport in networks with correlated velocity fields and more complex topologies.

We gratefully acknowledge funding for this research, provided by the DOE Office of Science Graduate Fellowship Program (to PKK), the Spanish Ministry of Science and Innovation (MICINN) through the project HEART (CGL2010-18450) (to MD), Eni S.p.A. under the Multiscale Reservoir Science project and the ARCO Chair in Energy Studies (to RJ).

[1] B. S. Kerner, Phys. Rev. Lett. **81**, 3797 (1998).
[2] D. Helbing, I. Farkas, and T. Vicsek, Nature (London) **407**, 487 (2000).
[3] M. Prakash and N. Gershenfeld, Science **315**, 832 (2007).
[4] I. Y. Wong, M. L. Gardel, D. R. Reichman, E. R. Weeks, M. T. Valentine, A. R. Bausch, and D. A. Weitz, Phys. Rev. Lett. **92**, 178101 (2004).
[5] B. Berkowitz and H. Scher, Phys. Rev. Lett. **79**, 4038 (1997).
[6] E. López, S. V. Buldyrev, S. Havlin, and H. E. Stanley, Phys. Rev. Lett. **94**, 248701 (2005).
[7] J. D. Noh and H. Rieger, Phys. Rev. Lett. **92**, 118701 (2004).
[8] L. K. Gallos, C. Song, S. Havlin, and H. A. Makse, Proc. Natl. Acad. Sci. USA **104**, 7746 (2007).
[9] A.-L. Barabási, Science **325**, 412 (2009).
[10] C. Nicolaides, L. Cueto-Felgueroso, and R. Juanes, Phys. Rev. E **82**, 055101(R) (2010).
[11] V. Colizza, R. Pastor-Satorras, and A. Vespignani, Nat. Phys. **3**, 276 (2007).
[12] H. Nakao and A. S. Mikhailov, Nat. Phys. **6**, 544 (2010).
[13] M. C. González, C. A. Hidalgo, and A.-L. Barabási, Nature (London) **453**, 779 (2008).
[14] J. Candia, M. C. González, P. Wang, T. Schoenharl, G. Madey, and A.-L. Barabási, J. Phys. A: Math. Theor. **41**, 224015 (2008).
[15] E. W. Montroll and G. H. Weiss, J. Math. Phys. **6**, 167 (1965).
[16] H. Scher and E. W. Montroll, Phys. Rev. B **12**, 2455 (1975).
[17] J. Klafter and R. Silbey, Phys. Rev. Lett. **44**, 55 (1980).
[18] R. Metzler and J. Klafter, Phys. Rep. **339**, 1 (2000).
[19] T. Le Borgne, M. Dentz, and J. Carrera, Phys. Rev. Lett. **101**, 090601 (2008).
[20] M. Dentz and A. Castro, Geophys. Res. Lett. **36**, L03403 (2009).
[21] E. Eisenberg, S. Havlin, and G. H. Weiss, Phys. Rev. Lett. **72**, 2827 (1994).
[22] M. Dentz, D. Bolster, and T. Le Borgne, Phys. Rev. E **80**, 010101(R) (2009).
[23] J. P. Bouchaud, A. Comtet, A. Georges, and P. Le Doussal, Ann. Phys. **201**, 285 (1990).
[24] B. Berkowitz, A. Cortis, M. Dentz, and H. Scher, Rev. Geophys. **44**, RG2003 (2006).